

# Fast Computation of First-Order Feature-Bispectrum Corrections

Peter Adshead<sup>1</sup> and Wayne Hu<sup>1,2</sup>

<sup>1</sup>*Kavli Institute for Cosmological Physics, Enrico Fermi Institute, University of Chicago, Chicago, IL 60637*

<sup>2</sup>*Department of Astronomy & Astrophysics, University of Chicago, Chicago IL 60637*

Features in the inflaton potential that are traversed in much less than an e-fold of the expansion can produce observably large non-Gaussianity. In these models first order corrections to the curvature mode function evolution induce effects at second order in the slow roll parameters that are generically greater than  $\sim 10\%$  and can reach order unity for order unity power spectrum features. From a complete first order expression in generalized slow-roll, we devise a computationally efficient method that is as simple to evaluate as the leading order one and implements consistency relations in a controlled fashion. This expression matches direct numerical computation for step potential models of the dominant bispectrum configurations to better than 1% when features are small and 10% when features are order unity.

## I. INTRODUCTION

Features in the inflaton potential can give rise to large non-Gaussianity [1, 2]. In order to also satisfy cosmic microwave background (CMB) constraints on the power spectrum, observability in the bispectrum of an individual feature requires that it be traversed when the horizon was of order the current horizon in a small fraction of an e-fold [3]. As this represents a strong violation of the slow-roll limit, corrections to the leading-order bispectrum expression can approach order unity. Curiously such models are in fact favored by the WMAP 7-year CMB power spectrum data and so further tests require more accurate techniques [3]. The improvement of the fit due to these models is not due to the glitch in the CMB data at  $\ell = 20 - 40$  [4-7], but comes predominantly from the region around first peak. Similar improvements have also been noted arising from transplanckian modifications to the power spectrum [8], axion monodromy inflation [9] and non-trivial initial vacuum choices [10]. While the polarization power spectrum is likely to provide the next test of such models [3, 11], the bispectrum of these models may also provide an important consistency check.

Features in the inflationary potential have a long history and have been considered by many authors going back to Starobinsky [12] who first calculated the power spectrum due to a potential with a discontinuous first derivative. The bispectrum due to such a feature was calculated by [13], see also [14]. The fluctuations in the power spectrum due to a step feature in the potential were considered by [15, 16] and their resulting non-Gaussian signatures in the bispectrum were calculated numerically by [1, 2] and an analytic approximation was found by [3, 17]. Steps in the warp factor and potential in the context of brane inflation were considered by [18]. Features in the power spectrum and large non-Gaussianities arising from resonant effects in the inflationary potential were first proposed by [2] and then discovered in axion monodromy inflation [9, 19, 20].

An exact calculation of the bispectrum for such models requires a computationally intensive direct integration of

the curvature fluctuations for each Fourier space configuration [1, 2] and is impractical for analysis purposes. In [17], a fast approximate method was developed based on the generalized slow roll (GSR) approach. Here the curvature fluctuation mode functions are iteratively corrected due to the presence of the feature. The leading-order expression was shown to be accurate to typically ten percent for small amplitude features and up to order unity for large amplitude features. In the small amplitude feature limit, this error is associated with slow-roll corrections that change the phase of the modefunctions [3]. Even without a feature, these corrections typically generate 10% changes to the bispectrum [21]. A full calculation of all first-order correction terms is computationally cumbersome [17] and again becomes impractical.

In this paper we show that the dominant first-order correction can be simply computed. In §II, we review the GSR approach and give all next to leading-order terms in the power spectrum and bispectrum. In §III, we isolate the dominant terms, test them against exact calculations, and establish their compatibility with power spectrum corrections in the squeezed limit. We discuss these results in §IV.

## II. GSR APPROXIMATION

In this section we review the GSR formalism [16, 22] for computing the power spectrum [23] and bispectrum [17] for inflationary models with relatively large amplitude features including next to leading-order corrections. Such corrections are first-order in the GSR iteration and second order in the deviations from slow-roll.

### A. Power Spectrum

Beyond the slow-roll approximation, the curvature power spectrum can be computed exactly in linear theory as

$$\Delta_{\mathcal{R}}^2 \equiv \frac{k^3 P_{\mathcal{R}}}{2\pi^2} = \lim_{x \rightarrow 0} \left| \frac{xy}{f} \right|^2, \quad (1)$$

where  $x = k\eta$  and  $\eta$  is the conformal time to the end of inflation. The modefunction  $y$  satisfies the Mukhanov-Sasaki equation,

$$\frac{d^2 y}{dx^2} + \left(1 - \frac{2}{x^2}\right) y = \frac{g(\ln x)}{x^2} y, \quad (2)$$

where

$$g \equiv \frac{f'' - 3f'}{f}, \quad (3)$$

with  $' \equiv d/d \ln \eta = d/d \ln x$  and

$$f = 2\pi z \eta = \sqrt{8\pi^2 \frac{\epsilon_H}{H^2}} a H \eta. \quad (4)$$

Here  $\epsilon_H$  is the slow-roll parameter

$$\epsilon_H \equiv \frac{1}{2} \left( \frac{d\phi}{d \ln a} \right)^2, \quad (5)$$

which is not necessarily small or constant. Throughout we set the reduced Planck mass  $M_{\text{pl}} = (8\pi G)^{-1/2} = 1$  as well as  $\hbar = c = 1$ . Note that  $f''/f$  in the source function  $g$  involves first derivatives of the second slow roll parameter

$$\eta_H = -\delta_1 \equiv \epsilon_H - \frac{1}{2} \frac{d \ln \epsilon_H}{d \ln a}. \quad (6)$$

Up to this point, no assumptions have been made beyond the validity of linear theory but the modefunction  $y$  remains an implicit functional of  $\epsilon_H$ . Briefly, the GSR approach to solving the modefunction equation (2) is to consider the RHS as an external source with an iterative correction to  $y$  [16]. To lowest order, we replace  $y \rightarrow y_0$  where

$$y_0 = \left(1 + \frac{i}{x}\right) e^{ix}, \quad (7)$$

is the solution to the equation with  $g \rightarrow 0$ . The first-order mode function  $y$  can then be obtained through the Green function technique. The result is an approximation that still requires  $\epsilon_H$  to be small in an absolute sense but allows it to evolve rapidly with large fractional changes to its value. Hence  $|g|$  can be large in an absolute sense.

To leading order, the curvature power spectrum is given by

$$\ln \Delta_{\mathcal{R}0}^2 = G(\ln \eta_*) + \int_{\eta_*}^{\infty} \frac{d\eta}{\eta} W(k\eta) G'(\ln \eta), \quad (8)$$

where  $k\eta_* \ll 1$  and

$$W(u) = \frac{3 \sin(2u)}{2u^3} - \frac{3 \cos(2u)}{u^2} - \frac{3 \sin(2u)}{2u}. \quad (9)$$

The source function for the power spectrum is given by

$$G = -2 \ln f + \frac{2}{3} (\ln f)', \quad (10)$$

and thus

$$G' = -2(\ln f)' + \frac{2}{3}(\ln f)'' = \frac{2}{3}g - \frac{2}{3}[(\ln f)']^2. \quad (11)$$

Note that the leading order expression for the power spectrum is already first-order in the deviations from slow roll.

The addition of the term quadratic in  $(\ln f)'$  to  $g$  in Eq. (11) makes  $G'$  a total derivative and guarantees that the power spectrum is independent of the arbitrary epoch  $\eta_*$  after horizon crossing, ensuring that the curvature remains constant thereafter [23].

To first order in the mode function iteration and second order in the slow-roll parameters [22, 23]

$$\Delta_{\mathcal{R}1}^2 = \Delta_{\mathcal{R}0}^2 \left\{ \left[1 + \frac{1}{4} I_1^2(k) + \frac{1}{2} I_2(k)\right]^2 + \frac{1}{2} I_1^2(k) \right\}, \quad (12)$$

where

$$\begin{aligned} I_1(k) &= \frac{1}{\sqrt{2}} \int_0^\infty \frac{d\eta}{\eta} G'(\ln \eta) X(k\eta), \\ I_2(k) &= -4 \int_0^\infty \frac{du}{u} \left[ X + \frac{1}{3} X' \right] \frac{f'}{f} F_2(u), \end{aligned} \quad (13)$$

with

$$F_2(u) = \int_u^\infty \frac{d\tilde{u}}{\tilde{u}^2} \frac{f'}{f}, \quad (14)$$

and

$$X(u) = \frac{3}{u^3} (\sin u - u \cos u)^2. \quad (15)$$

When  $f''/f$  controls the large deviations in  $G'$ , the dominant term is  $I_1$  [23]

$$\Delta_{\mathcal{R}1}^2 \approx \Delta_{\mathcal{R}0}^2 \{1 + I_1^2(k)\}. \quad (16)$$

For a wide range of models, this has been shown to be a good approximation when  $|I_1| \lesssim 1/\sqrt{2}$  [24]. In this approximation, the power spectrum depends only on a single source function  $G'$  through two single integrals over the functions  $W$  and  $X$ . We seek a similarly simple but accurate approximation for the bispectrum in what follows.

## B. Bispectrum

For models in which large slow-roll corrections arise from a sharp feature where  $\eta'_H$  or  $f''/f$  becomes large, the bispectrum can be approximated as [17]

$$\begin{aligned} B_{\mathcal{R}}(k_i) &= 4\Re \left\{ i \mathcal{R}_{k_1}(\eta_*) \mathcal{R}_{k_2}(\eta_*) \mathcal{R}_{k_3}(\eta_*) \right. \\ &\quad \times \left[ \int_{\eta_*}^{\infty} \frac{d\eta}{\eta^2} a^2 \epsilon_H (\epsilon_H - \eta_H)' (\mathcal{R}_{k_1}^* \mathcal{R}_{k_2}^* \mathcal{R}_{k_3}^*)' \right. \\ &\quad \left. \left. + \frac{a^2 \epsilon_H}{\eta_*} (\epsilon_H - \eta_H) (\mathcal{R}_{k_1}^* \mathcal{R}_{k_2}^* \mathcal{R}_{k_3}^*)' \Big|_{\eta=\eta_*} \right] \right\}, \end{aligned} \quad (17)$$

where the curvature fluctuation is given by

$$\sqrt{\frac{k^3}{2\pi^2}}\mathcal{R}_k = \frac{xy}{f}, \quad (18)$$

the shorthand convention  $k_i = k_1, k_2, k_3$ , and  $\eta_*$  is an epoch well after all modes have left the horizon.

Using the same iterative GSR approach to evaluate  $y$ , the bispectrum to first-order in the modefunction correction or second order in the slow-roll violation becomes [17]

$$B_{\mathcal{R}}(k_i) = \frac{(2\pi)^4}{4} \frac{\Delta_{\mathcal{R}0}(k_1)}{k_1^2} \frac{\Delta_{\mathcal{R}0}(k_i)}{k_2^2} \frac{\Delta_{\mathcal{R}0}(k_3)}{k_3^2} \times \int_{\eta_*}^{\infty} \frac{d\eta}{\eta} g_B(\ln \eta) [U_0 + U_{1A} + U_{1B} + U_{1C} + U_{1D} + U_{1E}](k_i \eta), \quad (19)$$

where the source

$$g_B(\ln \eta) = \frac{(\epsilon_H - \eta H)'}{f}. \quad (20)$$

The leading order response to this source comes from

$$U_0(k_i \eta) = \left( \frac{d}{d \ln \eta} + 3 \right) \Re[y_0(k_1 \eta) y_0(k_2 \eta) y_0(k_3 \eta)]. \quad (21)$$

The first-order correction terms again involve  $G'$  and  $f'/f$

$$\begin{aligned} U_{1A}(k_i \eta) &= \frac{I_1(k_3)}{\sqrt{2}} \left( \frac{d}{d \ln \eta} + 3 \right) \\ &\quad \times \Im[y_0(k_1 \eta) y_0(k_2 \eta) [y_0^*(k_3 \eta) + y_0(k_3 \eta)]] \\ &\quad + \text{cyc.}, \\ U_{1B}(k_i \eta) &= -\frac{1}{2} \int_{\eta}^{\infty} \frac{d\tilde{\eta}}{\tilde{\eta}} G'(\ln \tilde{\eta}) W(k_3 \tilde{\eta}) \\ &\quad \times \left( \frac{d}{d \ln \eta} + 3 \right) \Re[y_0(k_1 \eta) y_0(k_2 \eta) y_0^*(k_3 \eta)] \\ &\quad + \text{cyc.}, \\ U_{1C}(k_i \eta) &= \left[ -\frac{I_1(k_3)}{\sqrt{2}} + \frac{1}{2} \int_{\eta}^{\infty} \frac{d\tilde{\eta}}{\tilde{\eta}} G'(\ln \tilde{\eta}) X(k_3 \tilde{\eta}) \right] \\ &\quad \times \left( \frac{d}{d \ln \eta} + 3 \right) \Im[y_0(k_1 \eta) y_0(k_2 \eta) y_0^*(k_3 \eta)] \\ &\quad + \text{cyc.}, \\ U_{1D}(k_i \eta) &= -\frac{3}{4} \int_{\eta}^{\infty} \frac{d\tilde{\eta}}{\tilde{\eta}} G'(\ln \tilde{\eta}) \left( \frac{1}{k_3 \tilde{\eta}} + \frac{1}{(k_3 \tilde{\eta})^3} \right) \\ &\quad \times \left( \frac{d}{d \ln \eta} + 3 \right) \Im[y_0(k_1 \eta) y_0(k_2 \eta) \\ &\quad [y_0^*(k_3 \eta) + y_0(k_3 \eta)]] + \text{cyc.}, \\ U_{1E}(k_i \eta) &= -3 \Re[y_0(k_1 \eta) y_0(k_2 \eta) y_0(k_3 \eta)] \\ &\quad \times \frac{f'}{f} \left[ 1 - \frac{1}{2g_B} \left( \frac{f'}{f} \right)^2 \right], \end{aligned} \quad (22)$$

where  $\text{cyc.}$  denotes the 2 additional cyclic permutations of the  $k$  indices. This first-order expansion has been shown to be highly accurate even for large amplitude features but has the drawback that it is cumbersome to compute since the nested integrals in  $U_{1B-D}$  involve configuration dependent quantities [17].

### III. FAST BISPECTRUM COMPUTATION

While first-order corrections to the bispectrum for models with features are generally at least of order 10% and hence important for accurate computation, most of the first-order terms in Eq. (22) are irrelevant where the bispectrum is observably large. On the other hand some of these terms are important for maintaining physicality in the superhorizon and squeezed limits. In §III A and III B, we devise and then test a first-order methodology that both efficiently corrects the bispectrum where it is large and implements physicality constraints in a controlled fashion.

#### A. Methodology

An observably large bispectrum arises if potential features are sufficiently sharp that they are traversed in much less than a Hubble time. In this case, the dominant contributions to the bispectrum arise when the modes are well inside the horizon  $k\eta \gg 1$ . Even if the features themselves are of small amplitude, first-order corrections from the slow-roll contributions to  $G'$  make substantial fractional corrections to the bispectrum [3]. In this case  $G'$  is nearly constant and we can evaluate the expressions in Eq. (22). We derive our method from these two assumptions but show that the resulting expressions remain a good approximation even when features in the power spectrum reach order unity or when one of the sides of the triangle is outside the horizon.

Under these two assumptions, all the nested integrals contribute very little to the integrand in Eq. (19) in that most of their impact is around or after horizon crossing rather than before. In addition, models with large bispectra contribute mainly through the  $f''/f$  terms in  $g_B$  and  $G'$  and so  $U_{1E}$  is negligible. The remaining terms are the ones proportional to  $I_1(k)$  in  $U_{1A}$  and  $U_{1C}$ . In fact the  $y_0 y_0 y_0^*$  contributions of these two terms cancel exactly leaving only  $y_0 y_0 y_0$  contribution similar to the zeroth order term (21). As noted in [3], this fact means that for triangles where all three  $k\eta \gg 1$ , the first-order corrections can be cast in the same form as that of the zeroth order term, namely in terms of single integrals involving only the perimeter of the triangle  $K = k_1 + k_2 + k_3$ .

As  $k\eta$  decreases, the  $I_1$  and integral contributions to  $U_{1C}$  cancel, leaving the  $U_{1A}$  term as the dominant correction. However as  $k\eta \rightarrow 0$ , the other first-order corrections ensure that the bispectra remain constant in accord with conservation of the comoving curvature  $\mathcal{R}_k$ . This

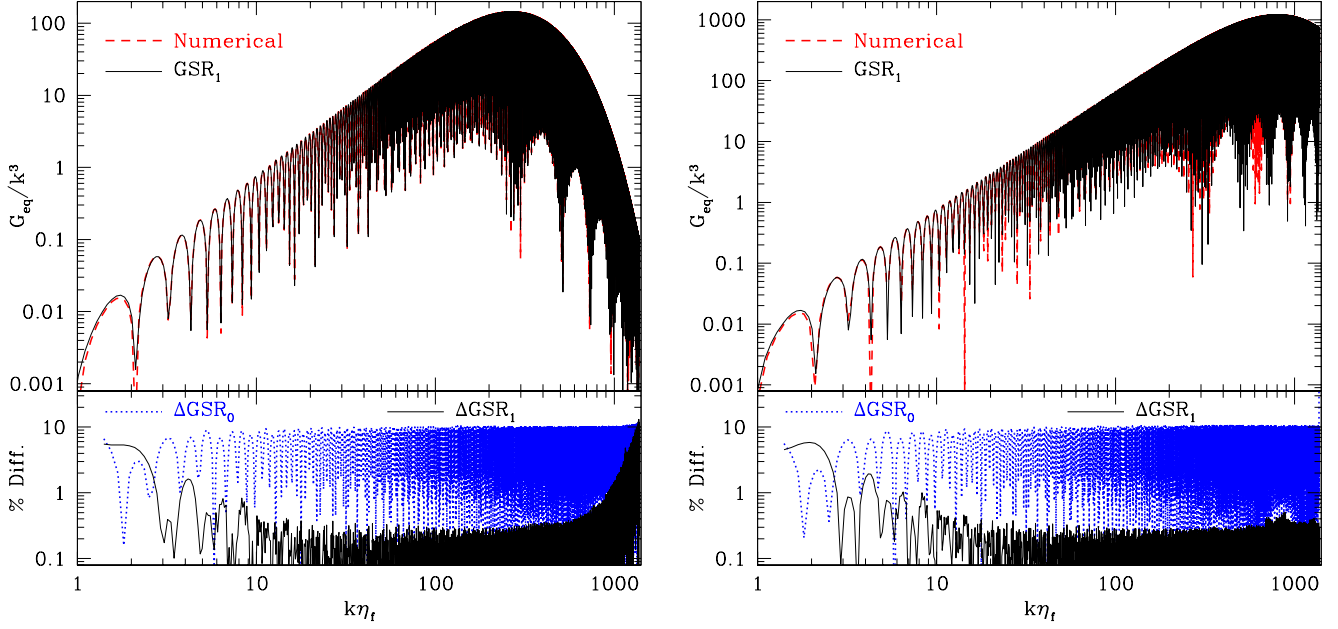


FIG. 1. Equilateral bispectrum for a small amplitude step  $c = 10^{-5}$  with  $d = 0.0001$  (left) and  $0.0003$  (right). Upper panel shows the  $\text{GSR}_1$  first order approximation versus the full numerical computation. Lower panel shows the percentage difference between the two as well as between the zeroth order approximation  $\text{GSR}_0$  and the numerical one.

condition can be alternately enforced by replacing the bispectrum source with a total derivative [17]

$$g_B \rightarrow G'_B(\ln \eta) = \left( \frac{\epsilon_H - \eta_H}{f} \right)', \quad (23)$$

just as in the case of the power spectrum. Combining these considerations, our fast first-order bispectrum expression becomes

$$\begin{aligned} B_{\mathcal{R}}(k_i) \approx & \frac{(2\pi)^4}{k_1^3 k_2^3 k_3^3} \frac{\Delta_{\mathcal{R}0}(k_1)\Delta_{\mathcal{R}0}(k_2)\Delta_{\mathcal{R}0}(k_3)}{4} \\ & \left[ -I_{B0}(K)k_1k_2k_3 - I_{B1}(K) \sum_{i \neq j} k_i^2 k_j \right. \\ & + I_{B2}(K)K \sum_i k_i^2 + \sum_m \frac{I_1(k_m)}{\sqrt{2}} \\ & \times \left( -I_{B3}(K)k_1k_2k_3 - I_{B4}(K) \sum_{i \neq j} k_i^2 k_j \right. \\ & + I_{B5}(K)K \sum_i k_i^2 \\ & + I_{B4}(K - 2k_m) \sum_{i \neq j} k_i^2 k_j (1 - 2\delta_{mj}) \\ & \left. \left. - (K - 2k_m)I_{B5}(K - 2k_m) \sum_i k_i^2 \right) \right], \quad (24) \end{aligned}$$

where

$$I_{Bn}(K) = G_B(\ln \eta_*) W_{Bn}(K\eta_*) + \int_{\eta_*}^{\infty} \frac{d\eta}{\eta} G'_B W_{Bn}(K\eta) \quad (25)$$

and

$$\begin{aligned} W_{B0}(x) &= x \sin x, & W_{B3}(x) &= -x \cos x, \\ W_{B1}(x) &= \cos x, & W_{B4}(x) &= \sin x, \\ W_{B2}(x) &= \sin x/x, & W_{B5}(x) &= -\cos x/x. \end{aligned}$$

The lack of a  $K - 2k_k$  term in  $I_{B3}$  comes from the  $x \gg 1$  cancellation of the  $U_{1A}$  and  $U_{1C}$  terms.

We shall call the  $n = 0 - 2$  terms the zeroth order approximation and the full set  $n = 0 - 5$  the first order approximation, denoting these  $\text{GSR}_0$  and  $\text{GSR}_1$  respectively. Note that the boundary term at  $K\eta_* \ll 1$  is formally only defined correctly for the  $n = 1, 2$  terms where  $W_{Bn} \rightarrow 1$  but we retain the others for notational compactness as their contributions vanish in this limit. While the  $I_{B5}$  term diverges as  $K\eta_* \rightarrow 0$  we shall see that the differencing construction in Eq. (24) guarantees that this divergence or the corresponding dependence on the arbitrary scale  $\eta_*$  has no observable consequence.

The computational cost of  $\text{GSR}_1$  is only double that of  $\text{GSR}_0$  involving 6 rather than 3 one dimensional integrals in addition to the power spectrum correction  $I_1(k)$  from Eq. (13). That the corrections are all proportional to  $I_1(k)$  is an important feature in our construction and we shall see enforces compatibility between the power spectrum and bispectrum approximations.

Although this construction is motivated by the slow-roll corrections to the bispectrum, we shall see next that it also works quite well for case where the correction is dominated by the feature itself.

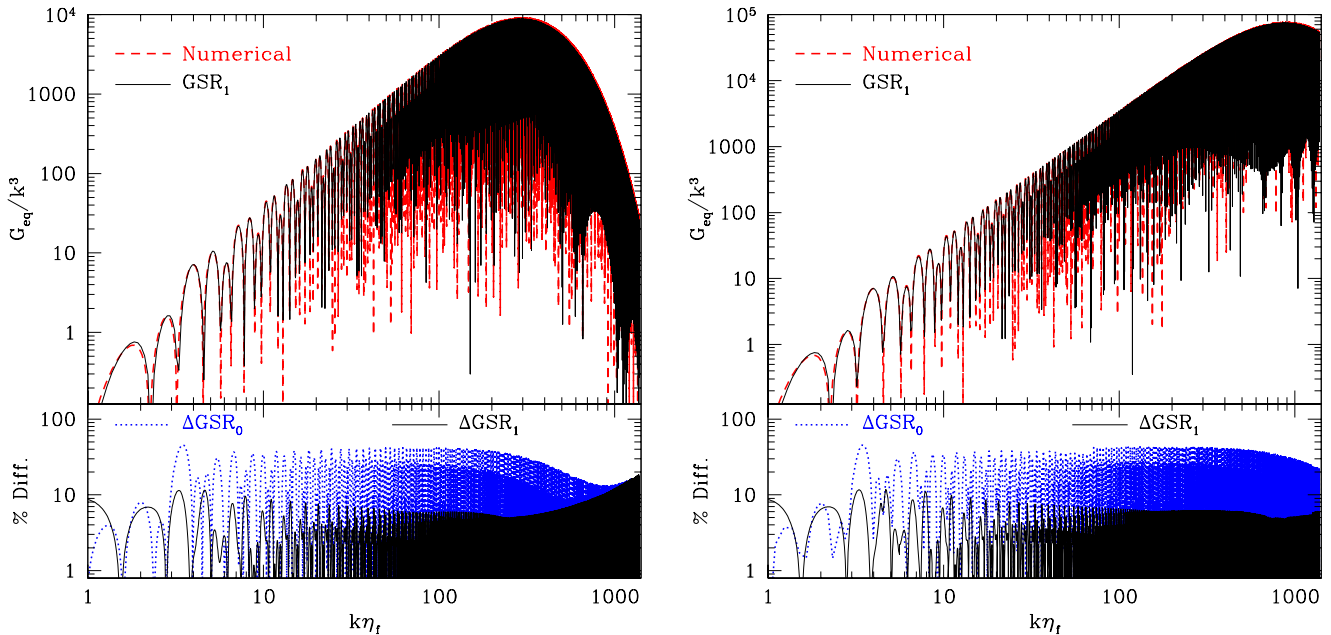


FIG. 2. Equilateral bispectrum for a large amplitude step  $c = 5.75 \times 10^{-4}$  with  $d = 0.0003$  (left) and  $0.0001$  (right). Upper panels shows the  $\text{GSR}_1$  first order approximation versus the full numerical computation. Lower panels shows the percentage difference between the two as well as between the zeroth order approximation  $\text{GSR}_0$  and the numerical one.

## B. Configuration Tests

As an example of a feature model with a possibly observable bispectrum, we consider the potential [15]

$$V(\phi) = \frac{1}{2} m^2 \phi^2 \left[ 1 + c \tanh \left( \frac{\phi - \phi_s}{d} \right) \right], \quad (26)$$

which corresponds to a smooth step at  $\phi = \phi_s$  of fractional height  $c$  and width  $d$ . Given the WMAP7 preference for a large scale feature, we set  $\phi_s$  to reproduce the scale of the maximum likelihood (ML) solution  $\eta(\phi_s) = 8.163$  Gpc [3]. For the amplitude, we take the case where  $c \rightarrow 0$  and the maximum likelihood solution for the WMAP7 data  $c = 5.75 \times 10^{-4}$ . For the width  $d$  we take several cases that would lead to observable bispectra with this amplitude and position. We choose  $m$  to be compatible with the WMAP7 slope for the underlying slow-roll potential  $m = 7.126 \times 10^{-6}$  such that the underlying tilt from the smooth part of the potential is  $\bar{n}_s \approx 0.963$ . Following the notation of the existing literature [1, 2], we construct the bispectrum statistic

$$\mathcal{G}(k_1, k_2, k_3) = \frac{k_1^3 k_2^3 k_3^3}{(2\pi)^4 \tilde{A}_S^2} B_{\mathcal{R}}(k_1, k_2, k_3), \quad (27)$$

where we take  $\tilde{A}_S = 2.39 \times 10^{-9}$  which is approximately the amplitude of the power spectrum in the absence of the feature.

Most of the observable impact of features in the bispectrum comes from equilateral triangles where  $k_1 \sim k_2 \sim k_3$

[3]. In this limit

$$B_{\mathcal{R}}(k, k, k) \approx \frac{(2\pi)^4 \Delta_{\mathcal{R}}^3(k)}{k^6} \frac{1}{4} \times \left\{ -I_{B0}(3k) - 6I_{B1}(3k) + 9I_{B2}(3k) + \frac{3I_1(k)}{\sqrt{2}} \left[ -I_{B3}(3k) - 6I_{B4}(3k) + 9I_{B5}(3k) + 2I_{B4}(k) - 3I_{B5}(k) \right] \right\}. \quad (28)$$

Note that

$$3I_{B5}(3k) - I_{B5}(k) = \int_{\eta_*}^{\infty} \frac{d\eta}{\eta} G'_B \left[ -\frac{\cos(3k\eta) - \cos(k\eta)}{k\eta} \right] \quad (29)$$

and so as  $k\eta \rightarrow 0$  the quantity in brackets vanishes and the expression becomes independent of the arbitrary end point  $\eta_*$ .

In Fig. 1 (upper), we compare the first order approximation ( $\text{GSR}_1$ ) to the full numerical calculation for the equilateral case and a small amplitude step  $c = 10^{-5}$  with  $d = 0.0001$  and  $0.0003$ . Differences in the upper panel are quoted as percentages of a smooth envelope

$$\frac{27}{4} \frac{c}{(\epsilon_0 + 3c)} \frac{\Delta_{\mathcal{R}0}^3(k)}{\tilde{A}_S^{3/2}} (k\eta_f)^2 \frac{k/k_D}{\sinh(k/k_D)}, \quad (30)$$

in the lower panel to avoid dividing by an oscillatory quantity. Here the equilateral damping scale

$$k_D = \frac{2}{3} \frac{\sqrt{2\epsilon_0 + 6c}}{\pi d \eta_f}, \quad (31)$$

and  $\epsilon_0 = 0.00925$  is the value calculated on the slow-roll background in the absence of the step. The form of the envelope is derived from the analytic solutions in [3] and is accurate at the several percent level for all models considered here.

For  $c = 10^{-5}$ , the agreement of  $\text{GSR}_1$  and the exact numerical treatment is excellent, with differences below the 1% level between the first oscillation and the damping scale set by the finite width  $d$  (upper panel). The first order correction eliminates the 10% errors of the  $\text{GSR}_0$  approximation that appear mainly as a phase error (lower panel). Deep in the damping tail, the first order solution develops a small phase difference leading to larger fractional errors but controlled amplitude errors. This error can be attributed to terms in the first order expansion at Eqn. (22) that are not captured by the approximation at Eqn. (24). In particular, contributions due to some of the nested integrals are damped more slowly than the leading order contributions. This means that deep in the damping tail they can become a significant fraction of the leading order result. However, since this effect only becomes important in the region where the bispectrum is already small, we conclude that it can be safely ignored.

This good agreement persists until the feature makes order unity changes to the power spectrum. In Fig. 2, we show the maximum likelihood amplitude model. Here the oscillations take on a modulated form where every third extrema is reduced in amplitude reflecting the strong oscillations in the power spectrum. These are well captured by the first order approximation between the first oscillation and the damping tail with residuals around  $\sim 6\%$  correcting the  $\sim 40\%$  errors of the zeroth order approximation. Errors in the damping tail grow again mainly due to a phase error but remain small until the bispectrum amplitude has damped to an unimportant level. Note that in this example the maximum of  $|I_1| \approx 0.25$ . Like the power spectrum, this quantity monitors the accuracy of the first order computation. The criteria for equilateral bispectrum is slightly more stringent than the power spectrum due to the 3  $k$ -modes that can be corrected and hence

$$|I_1| \lesssim \frac{1}{3\sqrt{2}} \quad (32)$$

is the rough criteria for better than 10% percent level accuracy.

An important check of the physicality of the bispectrum is the squeezed limit where  $k_1 = k_S \ll k_2 \approx k_3 = k_L$  and the the bispectrum must satisfy consistency with the power spectrum [25]

$$\begin{aligned} n_s(k_L) - 1 &\equiv \left. \frac{d \ln \Delta_{\mathcal{R}}^2}{d \ln k} \right|_{k_L} = - \frac{B_{\mathcal{R}}(k_S, k_L, k_L)}{P_{\mathcal{R}}(k_S)P_{\mathcal{R}}(k_L)} \\ &\equiv - \frac{12}{5} f_{\text{NL}}(k_S, k_L, k_L). \end{aligned} \quad (33)$$

Note that this is a non-trivial check on our construction even for small amplitude features since we retained only

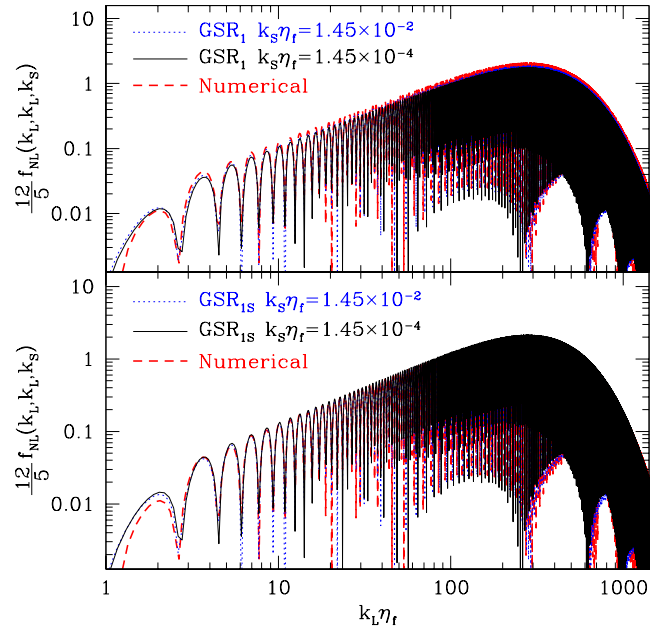


FIG. 3. Squeezed limit bispectrum for a step with small amplitude  $c = 10^{-5}$ ,  $d = 0.0003$ . Shown here is  $12f_{\text{NL}}(k_L, k_L, k_S)/5$  for various values of the short side,  $k_S$ . In the upper panel, we show the result of evaluating the first order approximation  $\text{GSR}_1$  versus the full numerical computation. The lower panels here show the slow roll  $k_S$  rescaling  $\text{GSR}_{1S}$  from Eq. (43).

the leading order corrections when all three modes are subhorizon scale during feature crossing.

For squeezed configurations, our first-order approximation (24) becomes

$$\begin{aligned} B_{\mathcal{R}}(k_S, k_L, k_L) &\approx \frac{(2\pi)^4 \Delta_{\mathcal{R}}(k_S) \Delta_{\mathcal{R}}^2(k_L)}{k_L^3 k_S^3} \frac{1}{4} \quad (34) \\ &\times \left\{ -2I_{B1}(2k_L) + 4I_{B2}(2k_L) + \frac{4I_1(k_L)}{\sqrt{2}} \right. \\ &\left. \times \left[ -I_{B4}(2k_L) + 2I_{B5}(2k_L) - \frac{k_S}{k_L} I_{B5}(k_S) \right] \right\}. \end{aligned}$$

Since

$$\begin{aligned} 2I_{B5}(2k_L) - \frac{k_S}{k_L} I_{B5}(k_S) &= \int_{\eta_*}^{\infty} \frac{d\eta}{\eta} G'_B \left[ -\frac{\cos(2k_L\eta)}{k_L\eta} + \frac{\cos(k_S\eta)}{k_L\eta} \right] \\ &\approx \int_{\eta_*}^{\infty} \frac{d\eta}{\eta} G'_B \left[ -\frac{\cos(2k_L\eta) - 1}{k_L\eta} \right], \end{aligned} \quad (35)$$

the expression becomes independent on the arbitrary end point  $\eta_*$ .

To check the consistency relation, it is useful to combine all of the terms to form a single integral over the

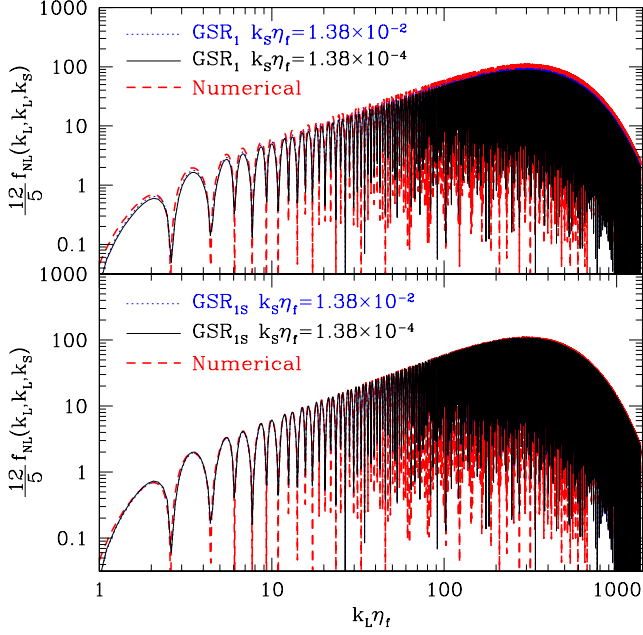


FIG. 4. Squeezed limit bispectrum for a step with large amplitude  $c = 5.75 \times 10^{-4}$  and  $d = 0.0003$ . Shown here is the GSR<sub>1</sub> and slow-roll corrected GSR<sub>1S</sub> approximations compared with the numerical computation as in Fig. 3. Note that the latter corrects all of the  $k_S$  dependent error.

source

$$B_{\mathcal{R}}(k_S, k_L, k_L) \approx \frac{(2\pi)^4}{k_L^3 k_S^3} \frac{\Delta_{\mathcal{R}}(k_S) \Delta_{\mathcal{R}}^2(k_L)}{4} I_{\text{sq}}(k_L), \quad (36)$$

where

$$I_{\text{sq}}(k) = G_B(\ln \eta_*) W_{\text{sq}}(k \eta_*) + \int_{\eta_*}^{\infty} \frac{d\eta}{\eta} G'_B W_{\text{sq}}(k \eta), \quad (37)$$

and

$$W_{\text{sq}}(x) = -2 \left[ \cos(2x) - \frac{\sin(2x)}{x} \right] - \frac{4I_1}{\sqrt{2}} \left[ \sin(2x) + \frac{\cos(2x) - 1}{x} \right], \quad (38)$$

with  $I_1 = I_1(k_L)$ . Using the approximation of Eq. (16) in the  $|I_1| \ll 1$  limit

$$\frac{d \ln \Delta_{\mathcal{R}}^2}{d \ln k} \approx \int d \ln \eta W'_P(k \eta) G'(\ln \eta), \quad (39)$$

where

$$W_P(x) = W(x) + \frac{2I_1}{\sqrt{2}} X(x). \quad (40)$$

To establish the consistency relation, we need to relate  $W_{\text{sq}}$  to  $W_P$  and  $G'_B$  to  $G'$ . We can manipulate the latter pair via integration by parts

$$\int_{\eta_*}^{\infty} d \ln \eta W'_P(x) G'(\ln \eta)$$

$$\begin{aligned} &= -2 \int_{\eta_*}^{\infty} d \ln \eta W'_P(x) \left[ \frac{f'}{f} - \frac{1}{3} \left( \frac{f'}{f} \right)' \right] \\ &= -2 \int_{\eta_*}^{\infty} d \ln \eta \frac{f'}{f} [W'_P + \frac{1}{3} W''_P] \\ &= 2 \frac{f'}{f} [W_P + \frac{1}{3} W'_P](x_*) \\ &\quad + 2 \int_{\eta_*}^{\infty} d \ln \eta \left( \frac{f'}{f} \right)' [W_P + \frac{1}{3} W'_P]. \end{aligned} \quad (41)$$

For bispectra that are dominated by  $f''/f$ ,  $G_B \approx -(f'/f^2)$ . If we further take the approximation that  $f \approx \Delta_{\mathcal{R}}^{-1} \approx \text{const.}$ , the consistency relation is satisfied since

$$2W_P + \frac{2}{3} W'_P = W_{\text{sq}}. \quad (42)$$

Thus the consistency relation holds in our first order bispectrum approximation as long as  $f$  remains nearly constant.

Of course  $f$  remains constant only at zeroth order in slow roll so there are additional correction in a full first order calculation. In Fig. 3 (upper), we show that correspondingly there is a small amplitude mismatch between the numerical and the GSR<sub>1</sub> results which grows logarithmically with decreasing  $k_S$ . Recall that the quantity  $f_{\text{NL}}(k_S, k_L, k_L)$  should become independent of  $k_S$  as  $k_S \rightarrow 0$  to satisfy the consistency relation.

One can gain further insight into the missing term by re-examining the slow-roll limit of the full first-order expression in Eq. (22) beyond the subhorizon approximation. Here  $G' \approx 1 - \bar{n}_s$ , where recall  $\bar{n}_s$  is the tilt that describes the power spectrum in the absence of the slow-roll violating feature. The leading contributions are from the  $U_{1B}$  and  $U_{1D}$  terms and account for the evolution of  $f$  between horizon crossing  $\eta \approx 1/k_S$ , when the curvature fluctuation for  $k_S$  froze out, and  $\eta_f$ , the epoch of slow-roll violation. They form a multiplicative correction to  $I_{1B}$  and  $I_{2B}$  of

$$R \approx \begin{cases} 1 + \frac{\bar{n}_s - 1}{2} \ln \left( \frac{k_S \eta_f}{x_{\text{max}}} \right), & k_S \eta_f < x_{\text{max}}, \\ 1, & k_S \eta_f \geq x_{\text{max}}, \end{cases} \quad (43)$$

with  $x_{\text{max}} = e^{2-\gamma_E}/2 \approx 2.07$  where  $\gamma_E$  is the Euler-Mascheroni constant. Note that the  $\ln(k \eta_f)$  term is simply the leading order slow-roll expansion of  $\Delta_{\mathcal{R}}(k_S)/\Delta_{\mathcal{R}}(\eta_f^{-1})$  as one might expect. Furthermore, the GSR technique can be shown to imply a slow-roll freeze out at  $k \eta = e^{7/3-\gamma_E}/2$  rather than  $= 1$  (see [16], Eq. 105). In Fig. 3 (lower), we demonstrate the effect of this rescaling with Eq. (43), denoted GSR<sub>1S</sub>. Here the  $k_S$  dependent discrepancy disappears entirely.

Applying this correction does not impact any triangle where all three modes are subhorizon at  $\eta_f$  and hence has very little impact on high signal-to-noise modes. Furthermore given that  $\eta_f$  must be comparable to the horizon size for the bispectrum features to be detectable in the



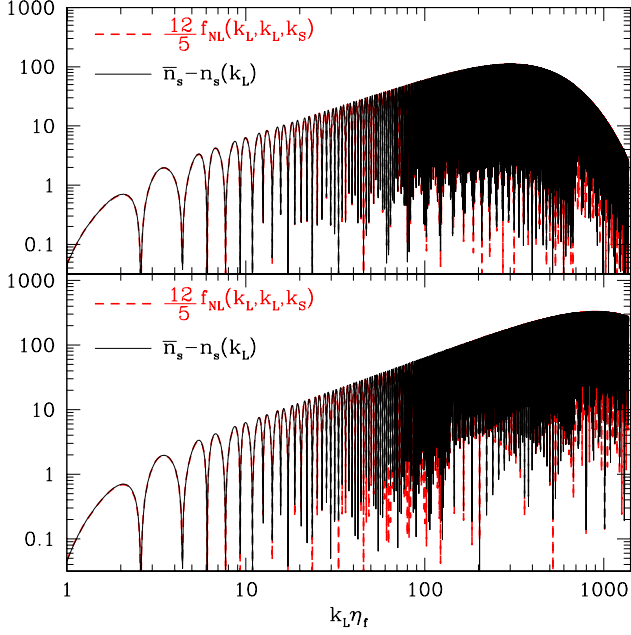


FIG. 5. Consistency relation test for a large amplitude step  $c = 5.75 \times 10^{-4}$  and  $d = 0.0003$  (upper) and  $0.0001$  (lower). Here the change in the power spectrum slope due to the feature  $\bar{n}_s - n_s$  and the squeezed bispectrum from the feature  $f_{NL}$  are both evaluated numerically. For the latter we take  $k_S \eta_f = 1.38 \times 10^{-2}$ , though the results are independent of this choice.

CMB, observable triangles cannot acquire large logarithmic corrections. We conclude that for practical purposes, this correction can be safely ignored.

At higher values of the step height,  $c$ , our scaling still removes the  $k_S$  dependent errors (see Fig. 4). This is because these errors correspond to the slow evolution of  $f$  between  $\eta = 1/k_S$  and  $\eta_f$  rather than the feature itself. On the other hand, a new scaling offset develops that can be attributed to the change the feature makes on  $f$  at  $\eta_f$ . In principle these could be corrected by integrating the feature contributions to  $G'$  in the first order  $U_{1B}$  and  $U_{1D}$  terms. However this offset is of the same order and nature as those found for the equilateral cases. Given that squeezed triangles do not dominate the signal-to-noise, we again conclude that further correction is unnecessary.

In Fig. 5, as a test of the consistency relation itself for a large amplitude step, we compare the numerical power spectrum slope to the squeezed bispectrum. The operator which dominates the bispectrum in the case of a feature is a subleading contribution to the usual slow-roll consistency relation. Thus, we subtract off the slow-roll contribution to the slope of the numerical power spectrum, and instead compare the squeezed limit bispectrum with the deviation away from the slow roll result for the slope of the power spectrum,  $\bar{n}_s - n_s(k_L)$ , where  $\bar{n}_s \approx 0.963$  is the slope of the power spectrum in the absence of the feature. In practice this correc-

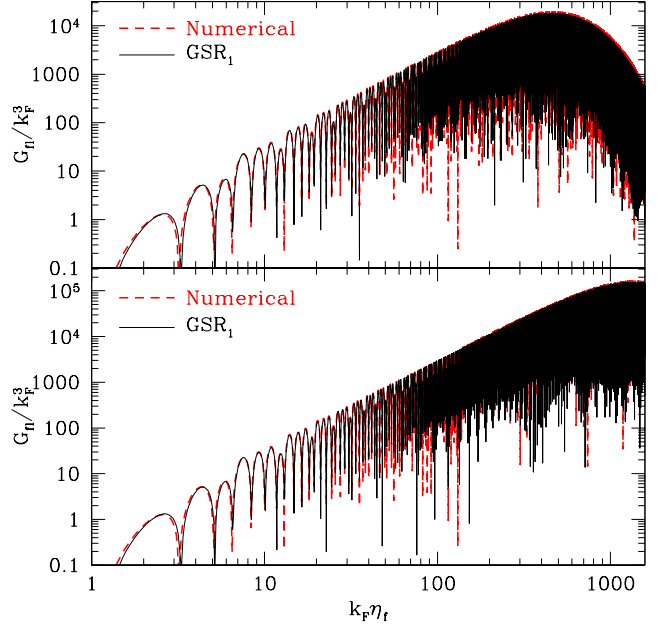


FIG. 6. Flat limit bispectrum for a large amplitude step  $c = 5.75 \times 10^{-4}$  with  $d = 0.0003$ . Flat triangle agreement between the  $GSR_1$  approximation and numerical evaluation is comparable to equilateral triangles.

tion is negligible if  $k_L \eta_f \gg 1$  or more generally when  $|f_{NL}| \gg \mathcal{O}(1 - \bar{n}_s)$ . It is only that the agreement is so good that we take it into account here. Furthermore, the excellent agreement checks the accuracy of the numerical bispectrum calculation.

Finally it is interesting to note that flat configurations where  $k_1 = 2k_2 = 2k_3 = k_F$  are somewhat special in Eq. (24), since the argument to the  $I_5$  integrals vanishes leaving the expression ill-defined. It is in fact well-defined if we take instead the limit of a flat triangle  $k_\epsilon = K - 2k_F \rightarrow 0$

$$\begin{aligned}
 B_{\mathcal{R}}(k_F, k_F/2, k_F/2) &\approx \frac{(2\pi)^4}{k_F^6} 4\Delta_{\mathcal{R}}(k_F) \Delta_{\mathcal{R}}^2(k_F/2) \\
 &\left\{ -I_{B0}(2k_F) - 7I_{B1}(2k_F) + 12I_{B2}(2k_F) \right. \\
 &+ \frac{I_1(k_F)}{\sqrt{2}} \left[ -I_{B3}(2k_F) - 7I_{B4}(2k_F) + 12I_{B5}(2k_F) \right. \\
 &\left. \left. - 6\frac{k_\epsilon}{k_F} I_{B5}(k_\epsilon) \right] \right. \\
 &+ \frac{2I_1(k_F/2)}{\sqrt{2}} \left[ -I_{B3}(2k_F) - 7I_{B4}(2k_F) + 2I_{B4}(k_F) \right. \\
 &\left. \left. + 12I_{B5}(2k_F) - 6I_{B5}(k_F) \right] \right\}, \tag{44}
 \end{aligned}$$

which again becomes independent of  $\eta_*$  as the triangle flattens. In Fig. 6, we compare our first order approximation to the numerical results. For scales between the first oscillation and the damping tail, the approximation cap-



tures the flat and equilateral bispectrum behavior comparably well.

#### IV. DISCUSSION

We have devised an efficient method to compute first-order corrections to the bispectrum of inflationary models with features. First order corrections to the bispectrum are generically at least  $\sim 10\%$  and can reach order unity for order unity features in the power spectrum.

Based on the GSR approach, we have shown that corrections in the high  $k$  limit, where the bispectrum amplitude is set well within the horizon, take on a simple form involving only single integrals over the slow-roll parameters. This limit is observationally important since it is here that the bispectrum can become large if the inflaton crosses a feature in the potential in much less than an e-fold of the expansion. We have constructed these corrections such that they implement consistency relations at low  $k$  in a controlled fashion.

Comparison with direct numerical computation of the bispectrum shows that the approximation works extremely well for the full range where the bispectrum is large. For cases where the zeroth order expressions deviate by 50%, the first order approximation deviates by less than 10%. These techniques should be useful for analyzing any model where inflaton potential features provide observably large non-Gaussianity.

#### ACKNOWLEDGMENTS

This work was supported in part by the Kavli Institute for Cosmological Physics at the University of Chicago through grants NSF PHY-0114422 and NSF PHY-0551142 and an endowment from the Kavli Foundation and its founder Fred Kavli. WH was additionally supported by U.S. Dept. of Energy contract DE-FG02-90ER-40560 and the David and Lucile Packard Foundation.

- 
- [1] X. Chen, R. Easther, and E. A. Lim, JCAP, **0706**, 023 (2007), arXiv:astro-ph/0611645 [astro-ph].
  - [2] X. Chen, R. Easther, and E. A. Lim, JCAP, **0804**, 010 (2008), arXiv:0801.3295 [astro-ph].
  - [3] P. Adshead, C. Dvorkin, W. Hu, and E. A. Lim, Phys.Rev., **D85**, 023531 (2012), arXiv:1110.3050 [astro-ph.CO].
  - [4] H. Peiris *et al.* (WMAP Collaboration), Astrophys.J.Suppl., **148**, 213 (2003), arXiv:astro-ph/0302225 [astro-ph].
  - [5] L. Covi, J. Hamann, A. Melchiorri, A. Slosar, and I. Sorbera, Phys. Rev., **D74**, 083509 (2006), arXiv:astro-ph/0606452.
  - [6] J. Hamann, L. Covi, A. Melchiorri, and A. Slosar, Phys. Rev., **D76**, 023503 (2007), arXiv:astro-ph/0701380.
  - [7] D. K. Hazra, M. Aich, R. K. Jain, L. Sriramkumar, and T. Souradeep, JCAP, **1010**, 008 (2010), arXiv:1005.2175 [astro-ph.CO].
  - [8] J. Martin and C. Ringeval, Phys.Rev., **D69**, 083515 (2004), arXiv:astro-ph/0310382 [astro-ph].
  - [9] R. Flauger, L. McAllister, E. Pajer, A. Westphal, and G. Xu, JCAP, **1006**, 009 (2010), arXiv:0907.2916 [hep-th].
  - [10] P. Meerburg, R. Wijers, and J. P. van der Schaar, (2011), arXiv:1109.5264 [astro-ph.CO].
  - [11] M. J. Mortonson, C. Dvorkin, H. V. Peiris, and W. Hu, Phys. Rev., **D79**, 103519 (2009), arXiv:0903.4920 [astro-ph.CO].
  - [12] A. A. Starobinsky, JETP Lett., **55**, 489 (1992).
  - [13] J. Martin and L. Sriramkumar, JCAP, **1201**, 008 (2012), arXiv:1109.5838 [astro-ph.CO].
  - [14] F. Arroja, A. E. Romano, and M. Sasaki, Phys.Rev., **D84**, 123503 (2011), arXiv:1106.5384 [astro-ph.CO].
  - [15] J. A. Adams, B. Cresswell, and R. Easther, Phys. Rev., **D64**, 123514 (2001), arXiv:astro-ph/0102236.
  - [16] E. D. Stewart, Phys. Rev., **D65**, 103508 (2002), arXiv:astro-ph/0110322.
  - [17] P. Adshead, W. Hu, C. Dvorkin, and H. V. Peiris, Phys.Rev., **D84**, 043519 (2011), arXiv:1102.3435 [astro-ph.CO].
  - [18] R. Bean, X. Chen, G. Hailu, S.-H. Tye, and J. Xu, JCAP, **0803**, 026 (2008), arXiv:0802.0491 [hep-th].
  - [19] R. Flauger and E. Pajer, JCAP, **1101**, 017 (2011), arXiv:1002.0833 [hep-th].
  - [20] L. Leblond and E. Pajer, JCAP, **1101**, 035 (2011), arXiv:1010.4565 [hep-th].
  - [21] C. Burrage, R. H. Ribeiro, and D. Seery, JCAP, **1107**, 032 (2011), arXiv:1103.4126 [astro-ph.CO].
  - [22] J. Choe, J.-O. Gong, and E. D. Stewart, JCAP, **0407**, 012 (2004), arXiv:hep-ph/0405155.
  - [23] C. Dvorkin and W. Hu, Phys. Rev., **D81**, 023518 (2010), arXiv:0910.2237 [astro-ph.CO].
  - [24] C. Dvorkin and W. Hu, Phys.Rev., **D84**, 063515 (2011), arXiv:1106.4016 [astro-ph.CO].
  - [25] J. M. Maldacena, JHEP, **0305**, 013 (2003), arXiv:astro-ph/0210603 [astro-ph].